

Ultrafast Charge Transfer Enhancement in CdS-MoS₂ via Linker Molecule

Matthew Ciesler, Han Wang, Shengbai Zhang, and Damien West

November 23, 2022

Department of Physics, Applied Physics and Astronomy, Rensselaer Polytechnic Institute, Troy, NY 12180

Abstract

Hybrid systems, which take advantage of low material dimensionality, have great potential for designing nanoscale devices. Quantum dots (QDs)—a 0D nanostructure—can be combined with 2D monolayers to achieve success in photovoltaics and photocatalytic water splitting. In such colloidal systems, ligand molecules such as cysteine play an important role in device performance. The role of the ligand molecule in these QD heterostructures is poorly understood. In this study, time-dependent density functional theory (TD-DFT) is employed in order to explore how the ligand affect the charge transfer at the ultra-fast timescale. We study the charge transfer dynamics in CdS-MoS₂ heterostructures both with and without an organic linker molecule. We find that the ligand molecule enhances the ultrafast charge transfer, and that electrons are preferentially transferred from CdS to MoS₂ as band alignment would predict. The electronic dynamics and time-evolved projection character are sensitive to the ionic temperature and excitation density.

1 Introduction

Within the emerging solutions for alternative energy sources, photovoltaics [1][2][3] and photocatalyzed water splitting [4][5][6] based on quantum dots (QDs) have great potential. In these third generation devices, the operational principle is that the QD absorbs light, creating photoexcited electrons and holes which differentiate to the electrode and counter-electrode respectively. This separation of charge is fundamental to the operation of the device, and so understanding the nature of this charge separation is critical to the understanding of these systems.

One important facet of the electron transfer process in these QD systems is the ultrafast dynamics [7][8][9][10]. At this timescale, the mechanism of photoexcited charge separation is important, together with the interaction with the QD surface and charge trapping states [11] [12]. In the case of bifunctional ligand molecules[13], the ligand is expected to play a role in enhancing the charge transfer. In this study, we focus on the ligand effects in a CdS/MoS₂ heterostructure, which (along with closely related systems such as CdSe/MoS₂) have seen success in photovoltaics, photocatalysis, and photodetection [14][15][16][17]. is a window into a relatively unexplored regime for for the colloidal QD system, because TD-DFT Time-dependent density functional theory (TD-DFT) can allow one to simulate these nanoscale systems at a timescale of femtoseconds, which can capture important charge transfer dynamics [18]. TD-DFT is well-suited to study dynamic

processes such as excitations [19], and real time integration schemes [20] are especially suited for studying photoexcitations [21]. From a theoretical standpoint, the Runge-Gross theorem [22] demonstrates that TD-DFT is an *ab initio* technique that, in principle, is as fundamental as the Schrödinger equation

2 Methods

For time-dependent DFT (TD-DFT) calculations, a modified version of the Spanish Initiative for Electronic Simulations with Thousands of Atoms (SIESTA) [23] software package was employed. The basis for this calculation is a linear combination of atomic orbitals (LCAO), consisting of double zeta plus polarization (DZP) orbitals. In calculations at a nonzero temperature, molecular dynamics (MD) are performed in an NVE ensemble (microcanonical ensemble), where the system is thermalized by giving the ground state atomic configuration an appropriate amount of kinetic energy, and then evolving the system over time. The timesteps used for dynamic simulations are 1 fs for MD, and 0.5 Rydberg time (0.024 fs) for TD-DFT.

Regarding the atomic structure (See Fig. 1) of the simulation, note that the thiol group of ligand molecules such as cysteine coordinates to surface Cd [24] [25] [26] in CdSe/CdS QDs. Due to this preferential binding, the Cd-terminated surface [27] plays an especially important role. On the other side of the heterostructure, the pristine MoS₂ surface is inert and is functionalized with a S vacancy. These S vacancies are relatively abundant

arXiv:2211.12133v1 [physics.comp-ph] 22 Nov 2022

in real MoS₂ samples [28] [29], and functionalization to this defect via an O atom has been previously reported [30]. Thus, the ligand will be bifunctional to CdS and MoS₂ via its S and O ends, respectively. This three-way heterostructure construction is similar to previous DFT simulations [31]. For lattice commensuration, we used a 4 × 4 cross-section of CdS combined with a 2√7 × 2√7 cross-section of MoS₂, and strained MoS₂ by 2.8%.

3 Results

Fig. 1 shows the atomic structures for the heterostructures used in the TD-DFT simulations. The 0K (300K) separated systems are constructed so that the CdS and MoS₂ films are relaxed (thermalized) separately and then combined afterwards, respectively. The density of states is also plotted in Fig.2. In all of the cases, as can be seen in the density of states, the doubly-coordinated cysteine ligand has its gap opened up by the interactions, and type-II alignment occurs between CdS and MoS₂, although for case (c) the gap between the CdS VBM and the MoS₂ CBM is very small. The DOS for the 300K systems are broadened compared to the 0K systems, and in the systems without a ligand molecule, the change in the dipole causes the alignment between CdS and MoS₂ to shift so that the HOMO-LUMO gap of the system increases.

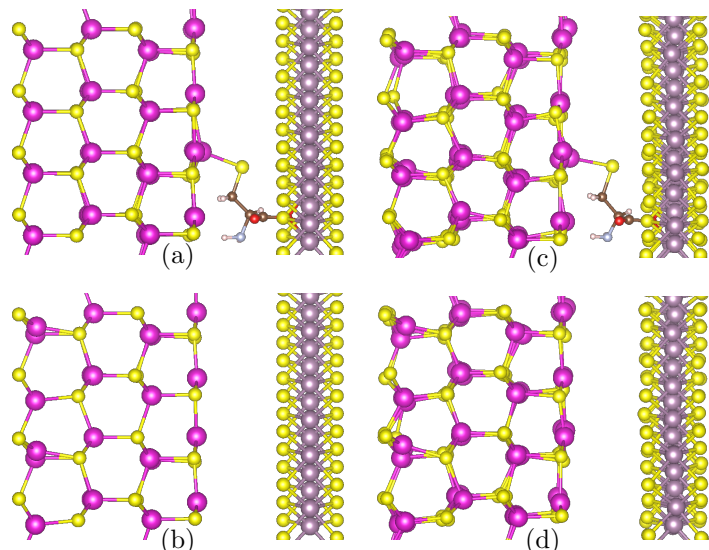


Figure 1: Atomic structure for the heterostructures used in TDDFT. The initial ionic temperature was (a-b) 0K and (c-d) 300K. The heterostructures are (a,c) CdS-Cys(*r*)-MoS₂-v_S and (b,d) CdS-MoS₂. Atoms: H (white), C (brown), O (red), N (blue), Cd (purple), S (yellow), Mo (grey).

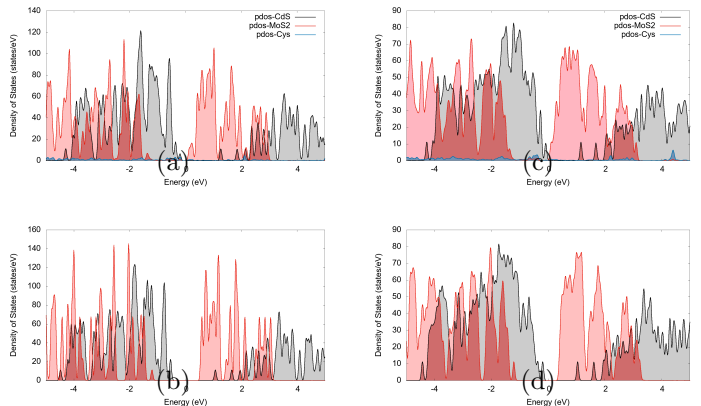


Figure 2: Density of states for the heterostructures used in TDDFT. The initial ionic temperature was (a-b) 0K and (c-d) 300K. The heterostructures are (a,c) CdS-Cys(*r*)-MoS₂-v_S and (b,d) CdS-MoS₂.

3.1 Results for 300 K Cys Heterostructures

Beginning with the 300K results, Table 1 shows the process for selecting the excitation states. One band is chosen as the excited electron state, which has to be empty initially, and another state for the hole, which is initially full. The criteria for the state to use is that the state should first and foremost be mostly projected onto CdS. This is because the excitation that the simulation is trying to mimic is a photoexcitation in CdS. But, as we see from the table, no state is purely CdS and there will always be a small amount of delocalization to Cys and MoS₂.

Band	CdS	Cys	MoS ₂	E (eV)	ID
806	98.8	1.0	0.2	-0.336	CdS VBM-3
807	99.5	0.4	0.1	-0.235	CdS VBM-2
809	88.7	6.0	5.2	-0.075	HOMO
810	2.4	8.9	88.7	0.056	LUMO
901	99.8	0.1	0.2	2.156	CdS CBM+2
902	99.2	0.3	0.5	2.207	CdS CBM+3

Table 1: Projection character (CdS, Cys, MoS₂, in percent), energy (E), and identity of states in the $T = 300K$ CdS-Cys(*r*)-MoS₂-v_S heterostructure.

Fig.3(a-c) shows the result for the first TD-DFT simulation. The excitation removes two electrons a CdS VB state and promotes it to a CdS CB state. At $t = 0$, we see from (a) that the energy level of the hole instantaneously decreases. This is a single-particle picture error, since the eigenfunctions will feel a new charge density. The hole is localized on the S-terminated surface of CdS, where it feels the gradient of the resulting dipole more than the delocalized hole state, which is why it is dis-

proportionately affected at $t = 0$. As time evolves, the hole evolves so that its eigenvalue increases, and the excited electron decreases in energy, according to expectations. The collective oscillations in the grey state (CdS VB states and MoS₂ CB states) are due to oscillating dipoles created by the movement of the charge density. Notice that when the MoS₂ CB band states move down in energy, their CdS VB counterparts move up in energy (and vice versa), since the dipole shifts the relative energy between the two.

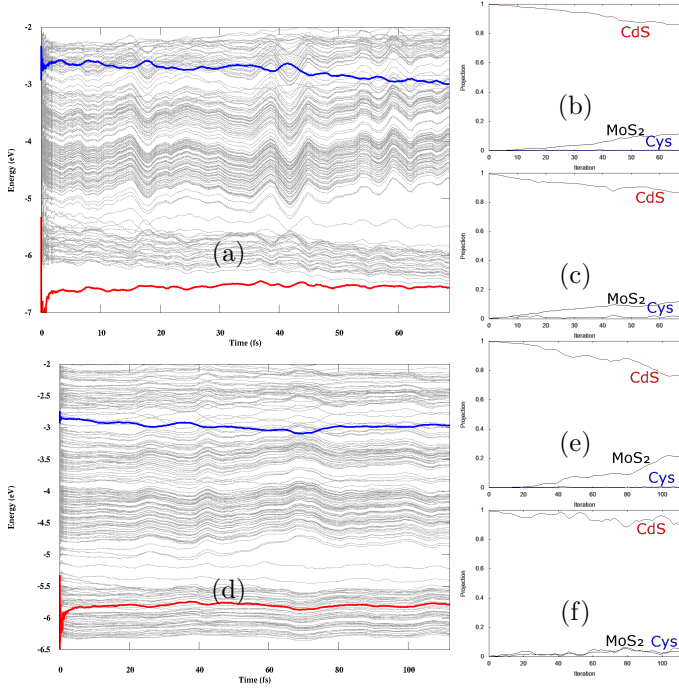


Figure 3: TD-DFT simulation of CdS–Cys(r)–MoS₂- v_S at T=300K. An excitation of $2.00e$ and $0.65e$ from the CdS VBM-2 to CdS CBM+2 was performed in (a-c) and (d-f), respectively. (a,d) Time evolution of the eigenvalues. VBM states below -6 eV are omitted. The blue line is the excited electron, and the red line is the excited hole. Projections (b,e)/(c,f) of the time-evolved electron/hole state, respectively, onto CdS, Cys, and MoS₂.

Looking at the plots of the projections (b-c), the excited electron state reaches 11.5% MoS₂ character, and the excited hole reaches 12.1% MoS₂ character. If we suppose that the evolution of these states mimics how photoexcited carriers would transfer, then 11.5% (12.1%) of the electron (hole) has transferred to MoS₂. This contradicts the expectations from band alignment, because based on the band alignment, the hole should not be able to transfer from CdS to MoS₂. The reason that it transferred anyway is due to the energy drop at $t = 0$. Looking at the density of states in Fig.2 (a), the MoS₂ valence band starts about 1.5 eV lower than the CdS VBM. This means that, at the energy the hole is actu-

ally at after $t = 0$, there *are* hole states nearby in energy that it can hybridize with.

For this reason, Fig.3(d-f) considers the same excitation but with a magnitude of 0.65. While the energy of the hole does still drop at $t = 0$, it does not cross into the MoS₂ VB states. The energy levels near the beginning of the simulation also indicate that the amount of energy the hole drops by is directly proportional to the magnitude of the excitation. This is consistent with the explanation that the drop in the hole energy is due to the change in the dipole, since the change in the dipole is proportional to the amount of charge displacement which is proportional to the magnitude of the excitation.

In Fig.3 (e-f), the electron transfers to MoS₂, but the hole does not. This is consistent with the previous observation about the position of the hole relative to the MoS₂ VB states. Note that the timescale for Fig.3(d-f) is larger than for Fig.3(a-c), so the transfer of the electron to MoS₂ has reached a larger value of 21.5%. Fig.4 shows a similar excitation to the previous one, with two differences: (i) the particular bands used in the excitation are different, but still have CdS projection character, and (ii) the length of the simulation is increased. The overall behavior of the simulation is similar to Fig.3(d-f), which gives evidence for the result not being sensitive to the particularly chosen excitation states, but rather their general character. By the end of the simulation, the electron had transferred 31.0% to MoS₂. Interestingly, some fluctuations in the projection of the hole onto Cys can be seen. But from these results, it isn't yet clear how the Cys is playing a role in the electron transfer. The projection plots show that the projection of the excited electron does not reach significant values throughout the simulation.

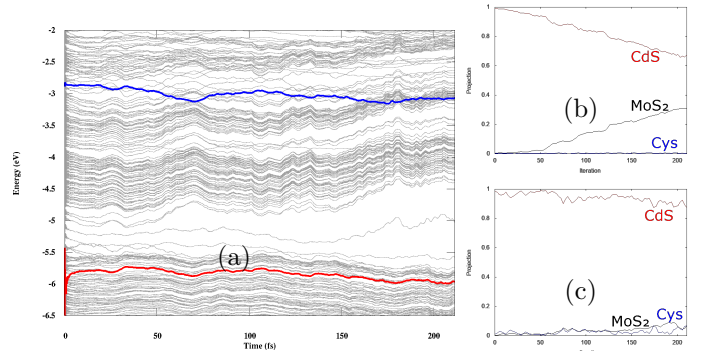


Figure 4: TD-DFT simulation of CdS–Cys(r)–MoS₂- v_S at T=300K. An excitation of $0.65e$ from the CdS VBM-3 to CdS CBM+3 was performed. (a-c) similar to Fig. 3(a-c).

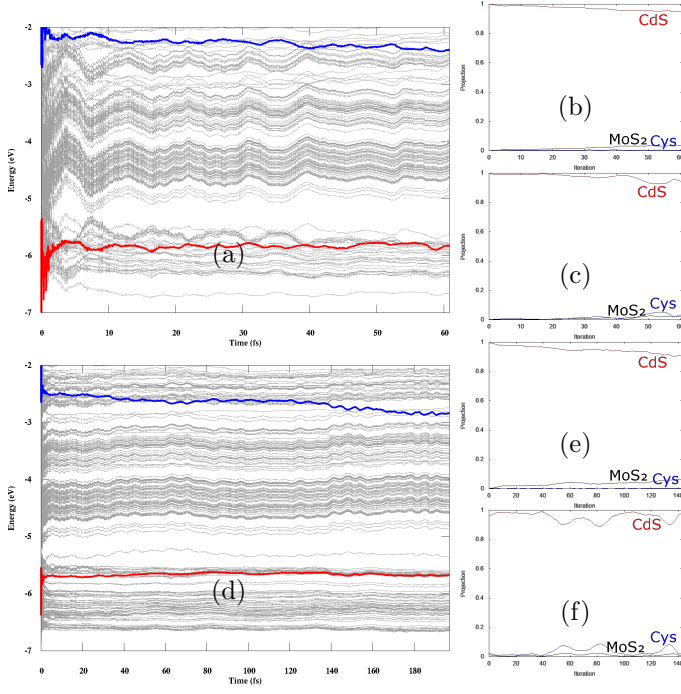


Figure 5: TD-DFT simulation of CdS–Cys(*r*)–MoS₂-*v*S at T=0K. An excitation of 2.00*e* and 0.65*e* from the CdS VBM-1 to CdS CBM+3 was performed in (a-c) and (d-f) respectively. (a,d) and (b-c,e-f) similar to Fig. 3.

3.2 Results for 0 K Cys Heterostructures

Fig.5 shows similar TD-DFT simulations for the T=0K system. Generally, we see that the magnitude of the charge transfer in the T=0K systems is less than the T=300K systems. For example, comparing Fig.5(e) with Fig.5(b), we see that at a similar total simulation time, the excited electron transferred nearly 40% in the 300K system but less than 5% in the 0K system. The differences in charge transfer rate may be due to the out-of-equilibrium atomic positions in the 300K system causing broadening in the density of states and subsequent coupling between these states. Another noticeable observation is that the magnitude of the hole energy drop is less in the 0K system than in the 300K system. It isn't clear why that should be the case, but similar observations have occurred in TD-DFT simulations of other systems [32]. Also, the lack of coupling causes coherent waves in the fluctuations of charge density, as seen from the relatively steady-frequency oscillations in Fig.5(a) and (d).

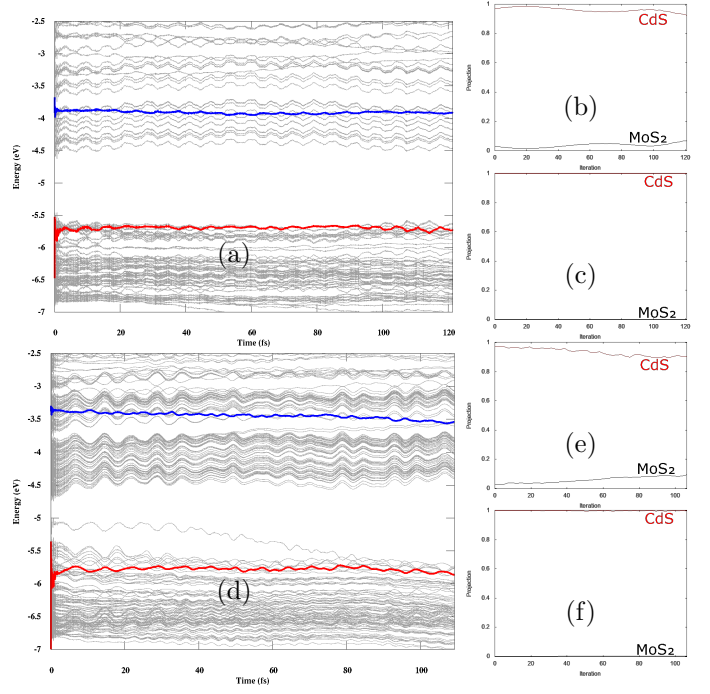


Figure 6: TD-DFT simulation of CdS–MoS₂ at T=0K and T=300K for (a-c) and (d-f) respectively. An excitation of 0.65*e* from the CdS VBM-1 (VBM-1) to CdS CBM (CBM+1) was performed in (a-c) and (d-f) respectively. (a,d) and (b-c,e-f) similar to Fig. 3.

3.3 Results for non-Cys Heterostructures

Next, we consider the simulation of systems that do not have a ligand molecule in the middle. The distance between the CdS and MoS₂ films was fixed to be same as the ligated heterostructures, namely 5.504 Å for the 0K system and 5.329 Å for the 300K system. In Fig.6, it is clear from the projection of the time-evolved electron (b,e) and hole (c,f) states that there is a significant reduction in the electron transfer rate. In fact, an imperceptible amount of the excited hole has transferred to MoS₂ in these systems, in contrast with the modest fluctuations seen in the ligated heterostructures. Comparing the electron transfer rates between the two systems, we see that the ligand enhances the electron rate by approximately a factor of 2.2. This enhancement may be underestimated due to the non-negligible MoS₂ projection of the initial acceptor state in the non-ligand TD-DFT simulations.

3.4 Conclusion

We find that TD-DFT successfully predicts the charge separation process seen in CdS heterostructures, namely that the excited electron in CdS transfers to MoS₂. This transfer rate is greater when the system is at an elevated ionic temperature, and is sensitive to

the dipole resulting from the photoexcited charge density and thus the cross-sectional excitation density. The charge transfer rates that are observed in heterostructures with the ligand molecule are greater than in the non-ligated counterparts by a factor of about 2.2.

While these TD-DFT simulations have successfully shown that the presence of the ligand molecule improves

the charge transfer, little time-evolved projection onto Cys was observed. One explanation is that the ligand density of states, which is hybridized with CdS and MoS₂ over a wide range of energies, effectively couples these states together, and this coupling has significant effects even if the magnitude of the coupling is small.

References

- [1] P. V. Kamat, "Quantum dot solar cells. the next big thing in photovoltaics," *J. Phys. Chem. Lett.*, vol. 4, no. 6, pp. 908–918, 2013.
- [2] N. Guijarro, Q. Shen, S. Giménez, I. Mora-Seró, J. Bisquert, T. Lana-Villarreal, T. Toyoda, and R. Gómez, "Direct correlation between ultrafast injection and photoanode performance in quantum dot sensitized solar cells," *J. Phys. Chem. C*, vol. 114, no. 50, pp. 22352–22360, 2010.
- [3] P. V. Kamat, "Boosting the efficiency of quantum dot sensitized solar cells through modulation of interfacial charge transfer," *Accounts Chem. Res.*, vol. 45, no. 11, pp. 1906–1915, 2012.
- [4] S. R. AR, H. M. Wilson, B. M. Momin, U. S. Annapure, and N. Jha, "Cdse quantum dots modified thiol functionalized g-c3n4: Intimate interfacial charge transfer between 0d/2d nanostructure for visible light h2 evolution," *Renew. Energ.*, vol. 158, pp. 431–443, 2020.
- [5] X. Luo, R. Li, K. P. Homewood, X. Chen, and Y. Gao, "Hybrid 0d/2d ni2p quantum dot loaded tio2 (b) nanosheet photothermal catalysts for enhanced hydrogen evolution," *Appl. Surf. Sci.*, vol. 505, p. 144099, 2020.
- [6] J. D. Benck, T. R. Hellstern, J. Kibsgaard, P. Chakthranont, and T. F. Jaramillo, "Catalyzing the hydrogen evolution reaction (her) with molybdenum sulfide nanomaterials," *Acs Catalysis*, vol. 4, no. 11, pp. 3957–3971, 2014.
- [7] J. Huang, D. Stockwell, Z. Huang, D. L. Mohler, and T. Lian, "Photoinduced ultrafast electron transfer from cdse quantum dots to re-bipyridyl complexes," *Journal of the American Chemical Society*, vol. 130, no. 17, pp. 5632–5633, 2008.
- [8] J. Huang, Z. Huang, Y. Yang, H. Zhu, and T. Lian, "Multiple exciton dissociation in cdse quantum dots by ultrafast electron transfer to adsorbed methylene blue," *Journal of the American Chemical Society*, vol. 132, no. 13, pp. 4858–4864, 2010.
- [9] Y. Yang, W. Rodriguez-Cordoba, X. Xiang, and T. Lian, "Strong electronic coupling and ultrafast electron transfer between pbs quantum dots and tio2 nanocrystalline films," *Nano letters*, vol. 12, no. 1, pp. 303–309, 2012.
- [10] S. Kaniyankandy, S. Rawalekar, and H. N. Ghosh, "Ultrafast charge transfer dynamics in photoexcited cdte quantum dot decorated on graphene," *The Journal of Physical Chemistry C*, vol. 116, no. 30, pp. 16271–16275, 2012.
- [11] A. J. Harvie, C. T. Smith, R. Ahumada-Lazo, L. J. Jeuken, M. Califano, R. S. Bon, S. J. Hardman, D. J. Binks, and K. Critchley, "Ultrafast trap state-mediated electron transfer for quantum dot redox sensing," *The Journal of Physical Chemistry C*, vol. 122, no. 18, pp. 10173–10180, 2018.
- [12] A. J. Goodman, N. S. Dahod, and W. A. Tisdale, "Ultrafast charge transfer at a quantum dot/2d materials interface probed by second harmonic generation," *The journal of physical chemistry letters*, vol. 9, no. 15, pp. 4227–4232, 2018.

- [13] D. V. Talapin, J.-S. Lee, M. V. Kovalenko, and E. V. Shevchenko, “Prospects of colloidal nanocrystals for electronic and optoelectronic applications,” *Chemical reviews*, vol. 110, no. 1, pp. 389–458, 2010.
- [14] F. A. Frame and F. E. Osterloh, “Cdse-mos2: a quantum size-confined photocatalyst for hydrogen evolution from water under visible light,” *J. Phys. Chem. C*, vol. 114, no. 23, pp. 10628–10633, 2010.
- [15] Y. Yuan, X. Zhang, H. Liu, T. Yang, W. Zheng, B. Zheng, F. Jiang, L. Li, D. Li, X. Zhu, *et al.*, “Growth of cdse/mos2 vertical heterostructures for fast visible-wavelength photodetectors,” *J. Alloy Compd.*, vol. 815, p. 152309, 2020.
- [16] Y. Wang, F. Zhang, M. Yang, Z. Wang, Y. Ren, J. Cui, Y. Zhao, J. Du, K. Li, W. Wang, *et al.*, “Synthesis of porous mos2/cdse/tio2 photoanodes for photoelectrochemical water splitting,” *Microporous and Mesoporous Materials*, vol. 284, pp. 403–409, 2019.
- [17] Y. Dong, Y. Chen, P. Jiang, G. Wang, X. Wu, R. Wu, and C. Zhang, “Efficient and stable mos2/cdse/nio photocathode for photoelectrochemical hydrogen generation from water,” *Chemistry—An Asian Journal*, vol. 10, no. 8, pp. 1660–1667, 2015.
- [18] G. Benkő, J. Kallioinen, J. E. Korppi-Tommola, A. P. Yartsev, and V. Sundström, “Photoinduced ultrafast dye-to-semiconductor electron injection from nonthermalized and thermalized donor states,” *Journal of the American Chemical Society*, vol. 124, no. 3, pp. 489–493, 2002.
- [19] A. Castro, H. Appel, M. Oliveira, C. A. Rozzi, X. Andrade, F. Lorenzen, M. A. Marques, E. Gross, and A. Rubio, “Octopus: a tool for the application of time-dependent density functional theory,” *physica status solidi (b)*, vol. 243, no. 11, pp. 2465–2488, 2006.
- [20] M. Huix-Rotllant, N. Ferré, and M. Barbatti, “Time-dependent density functional theory,” *Quantum Chemistry and Dynamics of Excited States: Methods and Applications*, pp. 13–46, 2020.
- [21] C. Lian, M. Guan, S. Hu, J. Zhang, and S. Meng, “Photoexcitation in solids: First-principles quantum simulations by real-time tddft,” *Advanced Theory and Simulations*, vol. 1, no. 8, p. 1800055, 2018.
- [22] E. Runge and E. K. Gross, “Density-functional theory for time-dependent systems,” *Physical review letters*, vol. 52, no. 12, p. 997, 1984.
- [23] J. M. Soler, E. Artacho, J. D. Gale, A. García, J. Junquera, P. Ordejón, and D. Sánchez-Portal, “The siesta method for ab initio order-n materials simulation,” *Journal of Physics: Condensed Matter*, vol. 14, no. 11, p. 2745, 2002.
- [24] D. F. Watson, “Linker-assisted assembly and interfacial electron-transfer reactivity of quantum dot- substrate architectures,” *J. Phys. Chem. Lett.*, vol. 1, no. 15, pp. 2299–2309, 2010.
- [25] S.-Y. Chung, S. Lee, C. Liu, and D. Neuhauser, “Structures and electronic spectra of cdse- cys complexes: density functional theory study of a simple peptide-coated nanocluster,” *J. Phys. Chem. B*, vol. 113, no. 1, pp. 292–301, 2008.
- [26] T. Kurihara, Y. Noda, and K. Takegoshi, “Capping structure of ligand–cysteine on cdse magic-sized clusters,” *ACS Omega*, vol. 4, no. 2, pp. 3476–3483, 2019.
- [27] J. Y. Rempel, B. L. Trout, M. G. Bawendi, and K. F. Jensen, “Density functional theory study of ligand binding on cdse (0001),(0001), and (1120) single crystal relaxed and reconstructed surfaces: implications for nanocrystalline growth,” *J. Phys. Chem. B*, vol. 110, no. 36, pp. 18007–18016, 2006.
- [28] H. Qiu, T. Xu, Z. Wang, W. Ren, H. Nan, Z. Ni, Q. Chen, S. Yuan, F. Miao, F. Song, *et al.*, “Hopping transport through defect-induced localized states in molybdenum disulphide,” *Nat. Commun.*, vol. 4, no. 1, pp. 1–6, 2013.
- [29] D. Liu, Y. Guo, L. Fang, and J. Robertson, “Sulfur vacancies in monolayer mos2 and its electrical contacts,” *Appl. Phys. Lett.*, vol. 103, no. 18, p. 183113, 2013.

- [30] J.-S. Kim, H.-W. Yoo, H. O. Choi, and H.-T. Jung, “Tunable volatile organic compounds sensor by using thiolated ligand conjugation on mos2,” *Nano Lett.*, vol. 14, no. 10, pp. 5941–5947, 2014.
- [31] M. Ciesler, D. West, and S. Zhang, “Ligand-assisted charge-transfer mechanism: The case of cdse/cysteine/-mos2 heterostructures,” *The Journal of Physical Chemistry Letters*, vol. 12, no. 51, pp. 12329–12335, 2021.
- [32] K. Cheng, H. Wang, J. Bang, D. West, J. Zhao, and S. Zhang, “Carrier dynamics and transfer across the cds/mos2 interface upon optical excitation,” *J. Phys. Chem. Lett.*, vol. 11, no. 16, pp. 6544–6550, 2020.